NATURAL CIRCULATION DEFROSTING IN FIN-AND-TUBE HEAT EXCHANGERS WITH HIGHLY DISTRIBUTED REFRIGERANT MASS FLOW

T. Oltersdorf, Dipl. Ing., S. Hoehlein, cand. B. Eng., J. Wapler, Dipl. Ing. (FH), H.-M. Henning, Dr., Thermal Systems and Buildings, Fraunhofer ISE, Heidenhofstraße 2, 79110 Freiburg, Germany

Abstract: The electrical energy demand for active defrosting of air-to-water heat pumps (HP) has been calculated from former HP field test monitoring results at Fraunhofer ISE. The share of electrical energy consumption of the compressor was determined at about 5 % per annum related to the overall heat energy. This energy demand can be decreased by using non-electric defrosting. One approach is natural circulation (NC) defrosting which reduces the electrical energy demand for defrosting to a minimum by using thermal energy from the sink. Electrical energy is thus only necessary for recovering the used heat as the driving force.

At our HP testbench with R1270 a fin-and-tube heat exchanger is operated as the evaporator with a cooling capacity of about 2 kW. Consequently to the configuration the pressure drop of the refrigerant distributor counteracts to the NC flow. We present results of some design issues regarding flow distribution and results of NC defrosting capacity applied to this evaporator. The evaporator is capable of using two different heat sources at the same time. Primarily this is air and subsequently a glycol-water-driven circuit.

Keywords: defrosting, heat pump, natural circulation, hydrocarbons, evaporator

1 INTRODUCTION

In all areas of heating, ventilation, air-conditioning and refrigeration (HVACR) vapour compression systems play a significant role for thermal energy transformation. In this highly competitive business systems comprising air-driven heat exchangers are dominating the market. Due to a demand in having compact and charge minimised refrigerant systems the design and optimization of evaporators is still of high scientific as well as economic interest which can be listed as follows:

(a) two-phase flow and fluid distribution in the supply line,
(b) frequent frosting and defrosting conditions during operation as well as cost-effective but efficient frost-detection systems,
(c) the interaction of these phenomena causing the need of the hydronic balancing of each refrigerant circuit in the case of a physical split-up of the flow and
(d) possible advances for compact designs and recyclability due to the optimization of classically designed fin-and-tube heat exchangers as well as the usage of other heat exchanger manufacturing technologies.

In this paper we focus on design issues for the two-phase refrigerant distribution as well as the application of non-electric defrosting techniques such as NC and its energy-saving potentials in comparison to the usage of reverse cycle defrosting which is dominant on the German market.

2 DESIGN ISSUES FOR FIN-AND-TUBE HEAT EXCHANGERS

The design selected for the investigated heat exchanger is different in the sense of applying a flow distributor to a HP system with a small heating capacity as needed for energy-efficient buildings. From the authors best knowledge there are four different solutions available on the market and several others are patented. Sorted according to its importance the four most relevant systems shown in figure 1 are based

(a) on the application of the venturi-effect (Tilney 1971),
(b) quite similar but more independent on the flow stratification at the inlet the nozzle distributor (Owens 1969),
(c) the so-called CAL distributor as invented by (Chawla and Schmitz 1977) and
(d) a newly introduced active distributor patented by (Mader et al. 2010).

It should be mentioned that only (a) and (b) are commonly used in refrigeration cycles in small capacity HVACR appliances. The devices (c) and (d) are usually addressing industrial process cooling and HP systems. Except (d) all devices are static. Air-to-water HP are often exposed to non-stable heat source and sink temperatures. In this case the mass flow is changing significantly. For these operation modes the distribution system needs to be stable.

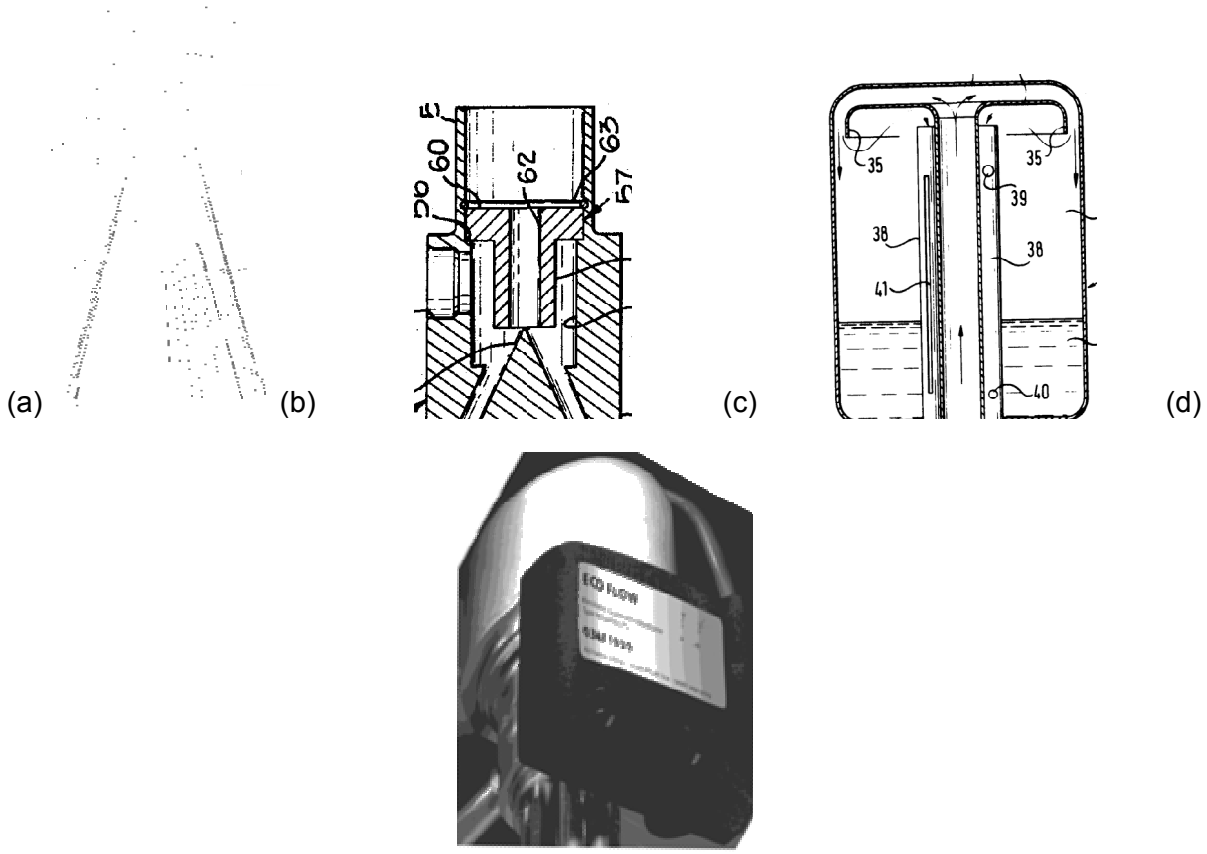

Figure 1: Survey on different flow distributors. (a) Venturi distributor as originally invented by Alco. (b) Nozzle distributor also with cone disperser and including a side-connection for hot gas bypass. (c) *CAL* distributor. It is a similar device to classical phase separators which is able to be manufactured as distributor with flash gas separation (not shown in the picture) or comprising a mixing process straight before the outlet of the device as presented below. (d) The only active device the so-called EcoFlow distributor. (No adequate patent picture given, see link at the end of the reference Mader 2010 for the given picture.)

This latter constraint causes the need of a detailed design of the static system and therefore the specified range in operation fits well into the stable mass flow range for well distributed flows. Thus (a) and (b) are the devices of choice for the investigated HP.

Referring to training material for refrigeration technicians/engineers (Reichelt) solution (a) is defined as the best solution for refrigerant distribution. However, reasons for the solution are not provided. Therefore a deeper analysis of the physical background is necessary to understand this "advice." The design procedure for the chain of devices throttle → distributor → distribution line → evaporator line with its pressure drop needs to be in the same size as the physically available pressure difference provided by the compressor. For the first design this is usually the pressure difference resulting from the nominal temperature levels of sink and source. Two important constraints limit the degrees of freedom in selecting all of these devices: (a) the evaporator tube register needs to be passed with small share in the overall pressure drop comprising the register itself and the distributor lines and (b) the available "free" pressure drop for throttling should not be too small in order to allow the usage of cost-efficient valves. Nowadays electronic expansion valves (EEV) are applied with pulse-wide modulation or step motors with very limited steps. The latter design leads to a very small operational range. Considering the criteria for the wide range of mass flows and thus changes in the pressure drop this is a very sensitive design issue.

Due to this fact the nozzle distributor usually causes higher pressure drops than venturi distributors. However, as mentioned before this device is much more independent of the inlet flow conditions whereas the flow conditions for venturi distributors should never become stratified. This is physically reasonable since the distribution effect depends significantly on the radial phase distribution before entering the venturi nozzle area. With state-of-the-art EEV the advantage of smaller needs in pressure drop for the distribution task becomes less important and thus the designer is more flexible in placing the distribution system in the upstream of the evaporator. According to (Sporlan Bulletin 2009) nozzle distributors should be designed for operation in-between 50-200 % of nominal cooling capacity of the system. To the best of the authors' knowledge selection and design software for distributors is very scarce. Only one software is known for nozzle distributors. This program uses constant pressure drops (0.17 MPa for the nozzle distributor and 0.07 MPa for the distribution lines). However, some aspects are not taken into account:

(a) additional degrees of freedom for the nozzle and the distributor line design due to the usage of EEV and
(b) high distribution of refrigerants even for small evaporators as a means to an end for saving refrigerant charge in classical fin-and-tube heat exchangers as evaporators.

To fulfil the above mentioned hydronic balancing for small capacity evaporators of each tube register the distribution lines need to be in capillary tube dimensions. The projected evaporator has a cooling capacity of 2 kW and was distributed by six registers. In this case the scarcely available design and selection software cannot be used since micro-scale models for heat transfer and for hydronic balancing the more important pressure drop is not modelled reasonably. The analysis of macro-to-microscale models is still actively investigated, i.e. (Thome 2004) for an overview of different criteria elaborated in the past to distinguish between macro- and micro-scale and (Revellin and Haberschill 2009) for present activities. A commonly accepted macro-to-micro-scale decision model was introduced (Kew and Cornwell 1997) as the threshold diameter d_{th} included in the definition of the dimensionless confinement number which is often also represented as the dimensionless Bond number. In this paper the given values represent the Bond number:

$$Bo = \frac{g \cdot \left(\rho_l - \rho_g\right) \cdot d_{th}^{\ 2}}{\sigma} \tag{1}$$

g is the gravitational acceleration, ρ is the liquid and gaseous density with the subscripts l and g and σ is the surface tension.

By applying the Bond number (1) it becomes obvious that the micro-scale needs to be taken into account since the threshold value of 4 is undercut by values between 0.8-1.1 at reasonable evaporation conditions in-between 250-280 K for the distribution lines. In the coaxial tube register which provides annuli for the refrigerant flow conditions are close to the Bond number of 4 with values in-between 4-5.3. Nevertheless for the design of the distribution lines as well as the estimation of the pressure drops in non-adiabatic parts of the tube register micro-scale models were applied.

The glycol-water circuit was also designed with six registers. For a suitable one phase fluid distribution manifold and collecting tubes were designed according to (Bassiouny and Martin 1984).

With this configuration the heat exchanger with staggered tubes and wavy fins is able to use glycol-water and air as heat sources parallel or separated, see figure 2, depending on the quality of the heat sources in terms of efficiency of the system or air-conditions concerning frost. The air-condition has a great impact on the following experiments since the system can be operated without downtimes. The annulus gap was designed to meet a pressure drop limiting the correlating change of the evaporation temperature to less than 1 K.

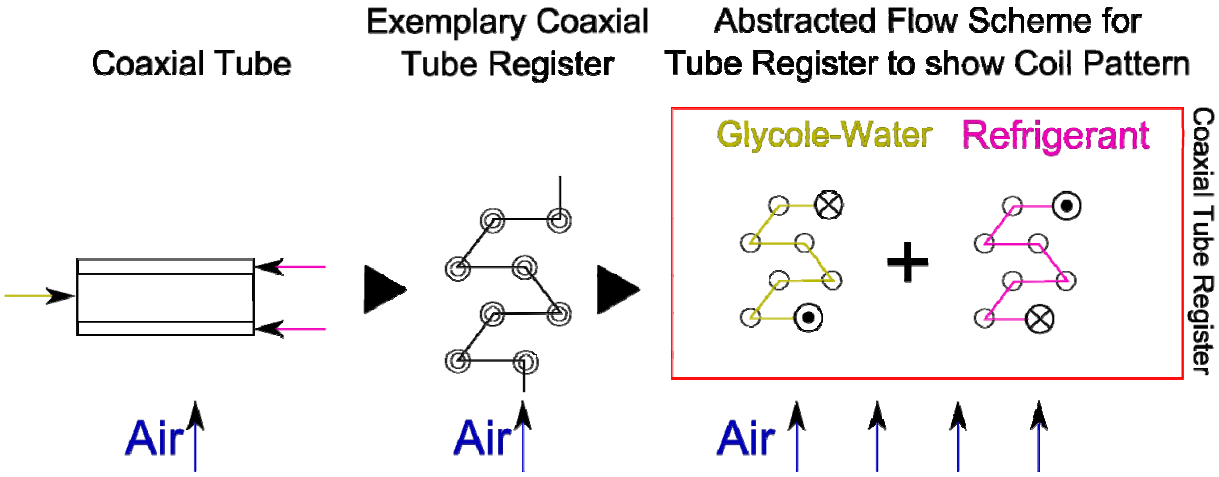

Figure 2: Simplified and conceptual analogy model of one coaxial tube register split into the flow in the inner tube (glycol-water) and the outer annulus (refrigerant) of the evaporator to visualise the applied flow scheme which is cross-current flow between refrigerant and air and pure counter flow between refrigerant and glycol-water. There is no direct thermal contact between air and glycol-water thus there is no efficiency loss due to thermal equilibration of potentially available higher quality source temperature levels. The red frame symbolises one of six coaxial tube registers.

3 DEFROSTING TECHNIQUES

Defrosting of air-driven evaporators were subordinate to important changes in the last three decades. Direct electric resistance heating elements and hot gas bypass defrosting were replaced by air-to-water HP applications to reverse cycles installed in a dominant share of residential HP. In recent monitoring projects the share for reverse cycle defrosting of the total amount of air-to-water HPs was more than 80 % for HPs in newly built houses (Miara et al. 2010) and even higher in existing houses (Hecking et al. 2008). Hot gas bypasses and

reverse cycle defrosting (Bertsch et al. 2002) were compared including effects related to the impact for defrosting at different operational temperatures and different ambient temperatures. Defrosting due to temperatures above the freezing point was also investigated.

Both, hot gas bypass defrosting as well as reverse cycle defrosting is cost-effective and easy to handle in terms of control design. Reverse cycle defrosting is usually much faster than hot gas bypass defrosting and contains a minor overall electrical energy demand (Bertsch et al. 2002). The high temperature level as well as the frequent reversal of condenser and evaporator can result in different problems (fogging and consequently ice formation in the air duct, chipping of ice plates which needs to be defrosted in the condensate pan, high thermal stresses due to frequent reversal usage of the heat exchangers and thus a decrease of life-time as well as higher risk in leakages). But in general the faster defrosting time and the minor electrical energy demand are main reasons for the prevalent application of reverse-cycle defrosting. (Miara et al. 2010).

The work from (Bertsch et al. 2002) also focused on passive defrosting and by using hot refrigerant from the accumulator after regularly stopped HP operation cycles but not on NC. Another promising defrosting technique above freezing point was presented by (Wellig et al. 2008). They have used active ventilated evaporators in the critical temperature range from 2°C to 7°C in which the most harmful frost/ice formation takes place. Additionally to the passive defrosting a small share of convective forces as well as the latent heat energy of the air humidity is used.

Natural circulation defrosting is already a topic for other researchers for HPs (Mildenberger 2008) but these works were limited to analysis with CO_2 and no evaporator design was applied which can have high impact on the performance of NC systems. In this work we focus on the investigation of this latter NC defrosting technique.

Table 1 presents these defrosting technologies and gives more information regarding the potentials and time necessary for defrosting. The potential is defined as a relative performance figure with hot gas bypass defrosting as the reference method. These data take the impact of pressure losses and thermal conduction losses inside the 4-way valve as well as heat loss in the heat sink into account.

Table 1: Survey on different defrosting technologies

Defrosting technique	Driving force	Energy demand [%]	Comments	Duration [min]	Reference	Operational limits
Hot gas bypass	Electrical Energy	100	State-of-the-art, inefficient	> 15	(a)	
Reverse cycle	Thermal and electrical energy	≈ 80	State-of-the-art, possibly harmful for the systems life-cycle, high defrosting capacity	< 10	(a)	
Passive air	Environmental thermal energy	< 10	State-of-the-art, time consuming	> 60	(b)	t_{amb} > 0 °C

Active air with follow-up operation of the ventilator	Environmental thermal energy and small share in electrical energy for ventilation and control	< 70	Non-standard, difficult control strategy, defrosting time depending on air moisture, only compatible with reverse cycle defrosting	5 < x < 40	(b)	t_{amb} > 0 °C
Natural circulation	Thermal energy from hot water	< 40	Non-standard, difficult in design phase	5 < x < 25	(a), (c), this work	T_{diff} between storage and evaporator > 15 K

The labelling in “References” represents (a) (Bertsch et al. 2002), (b) (Wellig et al. 2008) and (c) (Mildenberger 2008).

4 EXPERIMENTAL DESCRIPTION OF THE NC SYSTEM

The experimental investigation was conducted at the HP laboratory at Fraunhofer ISE, presented detailed in figure 3. The NC system was designed roughly by applying general design rules. No theoretical investigation except hydronic balancing of the tube system was conducted.

The NC system is shown in figure 4. To avoid too much expend effort the available evaporator test bench was extended by the additional circuit in which the spiral heat exchanger (SPHX) defines the thermal contact between the evaporator and the insulated water bath which simulates water storage. It was assumed that no change in flow direction change could occur due to the configuration with the collector tube at the nominal outlet of the evaporator. Here the annulus gap followed by the distribution line and nozzle distributor begins with a local maximum in height combined with relative large inner diameter which causes small local retention times of the fluid.

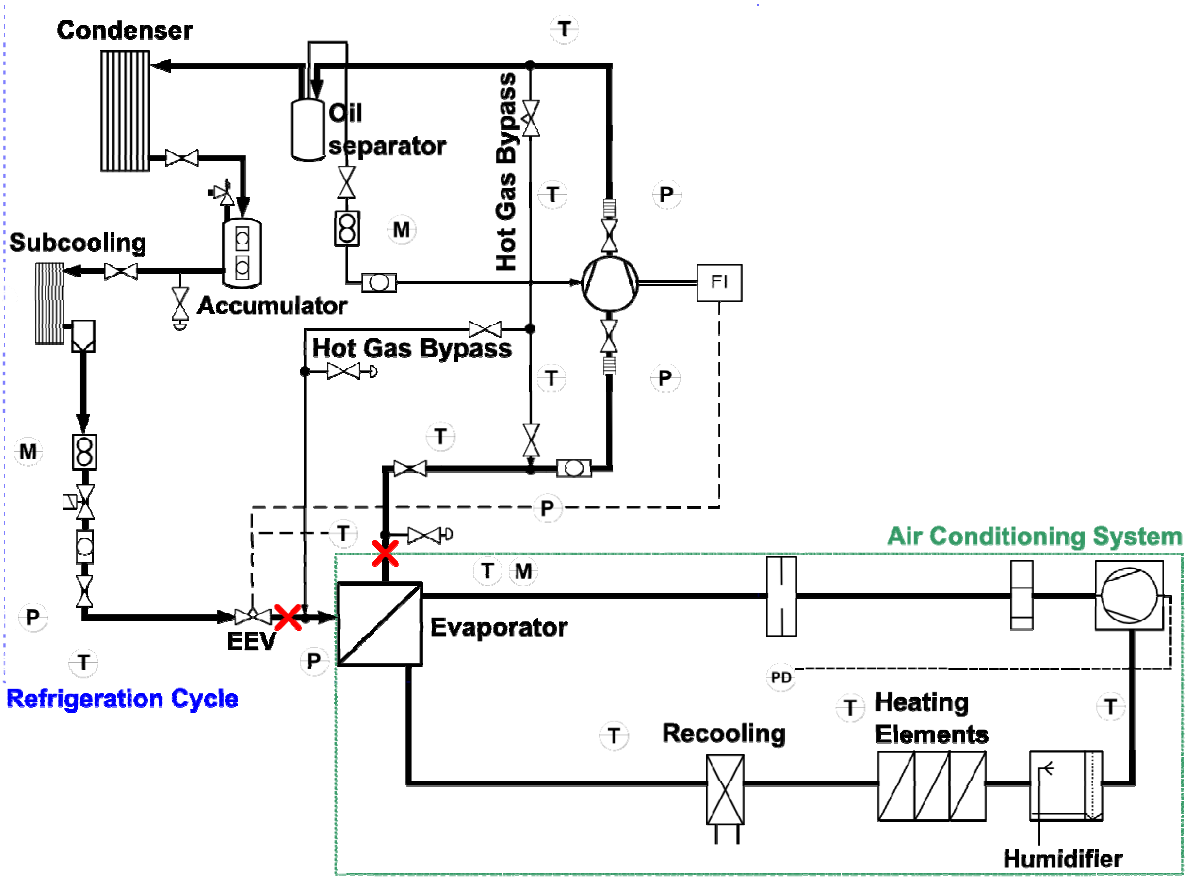

Figure 3: Scheme for the test bench at which the evaporator testing takes place. Air as heat source can be simulated in-between a volume flow range of 80-1400 m³/h. The refrigerant cycle is designed for the usage of R290 and R1270 as refrigerants and is able to test evaporators with a cooling capacity in-between 1.0-6.5 kW. The interconnection with the NC circuit is marked by the crosses.

The inner volume of the new circuit is 0.26 litres and the evaporator has 0.49 litres. The entire NC circuit has some additional inner volume for connecting tubes not presented in this scheme but used for charge calculation as pictured in figure 9. Flow direction design was further supported by insulating the downstream as deep as possible to avoid rising bubbles due to starting evaporation in this tube segment. The inlet to the SPHX is about 2.9 m long and comprises several horizontal levels of tube directions. The SPHX itself has 7.25 revolutions, a radius of 0.09 m and an overall height of 0.011 m. The outlet line has a total length of 1.5 m before entering the fluid distributor, which is furthermore equipped with several horizontal level tube segments. All connecting lines including the SPHX itself have an inner diameter of 5 mm.

Natural circulation takes place in the downtime period for the defrosting of the evaporator. The evaporator is operated nominally until the targeted frost conditions are met. Due to the small inner volumes of the tube system adjacent to the SPHX the capacity for refrigerant within this line was too small to “charge” the system sufficiently high to reach necessary pressure levels for a follow-up of NC operation. Thus a method was elaborated to charge the NC system externally via the EEV until a sufficient charge and thus pressure level was reached. The frost conditions in the evaporator were maintained by glycol-water and air-to-water temperatures below the freezing point. During the charging-period the evaporator remained cut of off the rest of the system to avoid unwanted buoyancy effects.

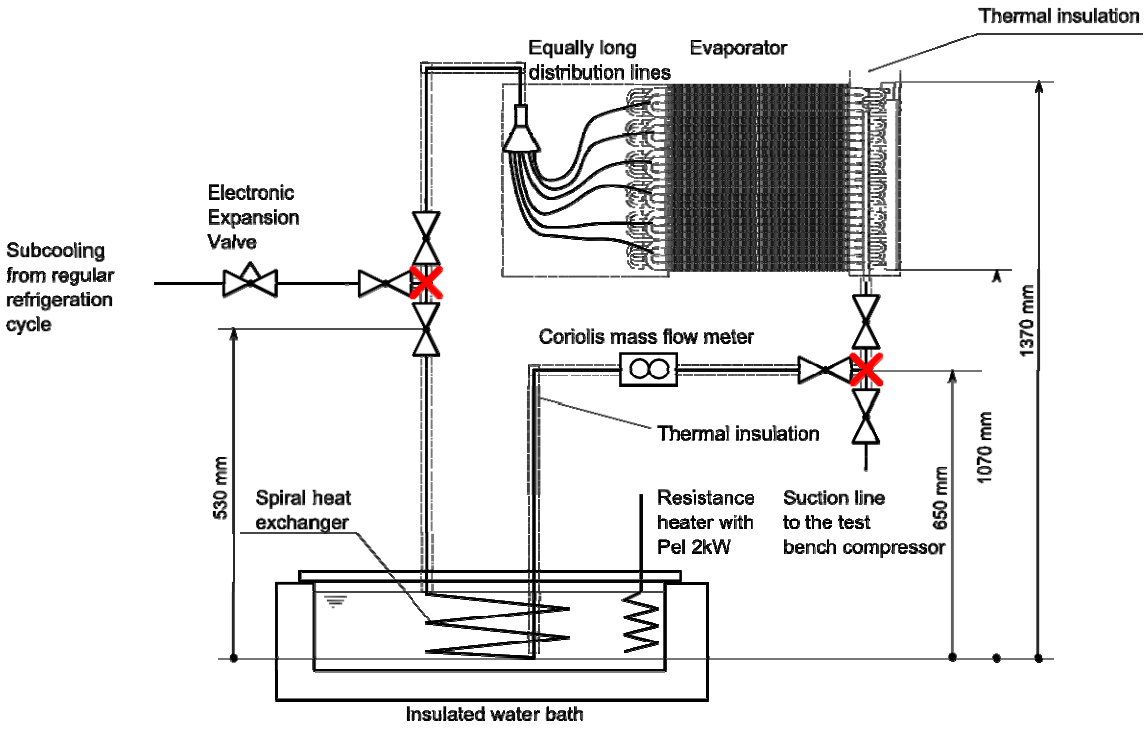

Figure 4: Illustration of the applied NC system. The insulated water bath simulates heated water storage. To have small local minima in which refrigerant is accumulated three ball valves are used. The flow direction of the NC circuit is intentionally not marked here but it was designed as a clock-wise circulation from the reader's point of view. See more details in the text. The red crosses symbolise the connection to the nominal refrigeration cycle.

Once the NC becomes active it is necessary to determine what optimization needs to be effected for the maximum in condensing capacity, which is to observe in figure 5. It is easy to identify with very few experiments if a NC system needs to be re- or discharged with refrigerant. In our experiments this orientation was used to locate our NC's capacity.

5 EXPERIMENTAL RESULTS

Experiments are mainly assigned to the investigation of the NC system. In this process an additional characteristic of this specific evaporator was investigated. First the results which are not related to NC are presented.
In figure 6 it can be seen that the HP operation does not stop. and with reaching a high temperature level of the secondary heat source the conditions for passive defrosting on the air side are provided after 50 minutes. The glycol-water circuit in this time operates with relatively high temperatures.

Of course this operation mode depends totally on the availability of high temperatures within the heat source connected to the glycol-water circuit. Thus it is obligatory that this heat source needs to be solar-thermal at a temperature level at which the necessary source capacity for a continued operation can be provided. This effect seems to be an interesting feature for solar-assisted HP systems in which the solar-thermal collector up to today only provides domestic hot water.

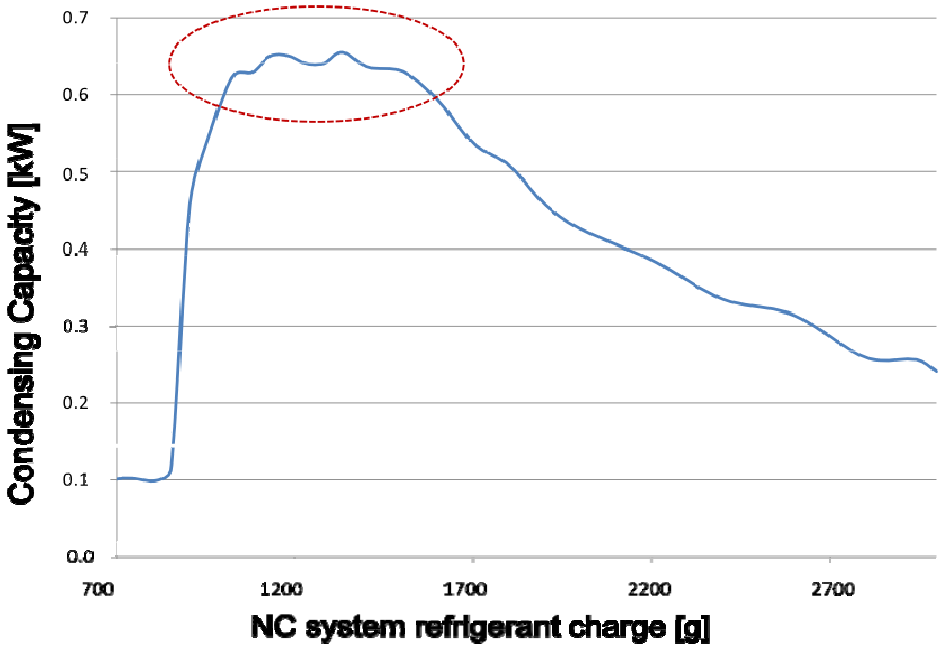

Figure 5: An exemplary condensing capacity of a NC system in which the maximum is reached in a small range of charge (Mildenberger 2008).

Recently experiments for the determination of optimal charging of the system started. The determination of the optimal charge level is very complex due to the fact that pressure levels at which NC takes place are only reached by filling the SPHX circuit of the overall NC cycle incrementally. Just by exposing the system to a temperature potential between the water bath and the evaporator at different pressure levels allowed quickly starting points for optimization. One of these charges is shown in figure 7 and figure 8. Immediately after reaching the two phase pressure levels correlating with the temperature levels exposed at water bath and evaporator, the NC cycle started.

The temperature in the evaporator is controlled at the freezing point level by examining the conditions of air and the glycol-water circuit. Almost every hour the water bath temperature shown at the y-axis is increased to evaluate a critical temperature range at which the defrosting starts. The numbers are provided as link for the following log (p)-h-diagram to simplify the understanding of the characteristics of the NC cycle.

The incremental change of the temperatures leads to a growing temperature gap in-between the SPHX outlet and the evaporator inlet temperature. As a result of superheated conditions and thermal energy losses in the tube section between SPHX and evaporator the highest temperature level is accompanied by the largest gap. This information and the knowledge on the pressure level at the same physical location reveals the NC cycle within the log(p)-h-diagram. Only for temperature level 6 superheated conditions are reached.
Condensed information of our NCs capacity at different charges is presented in figure 9.

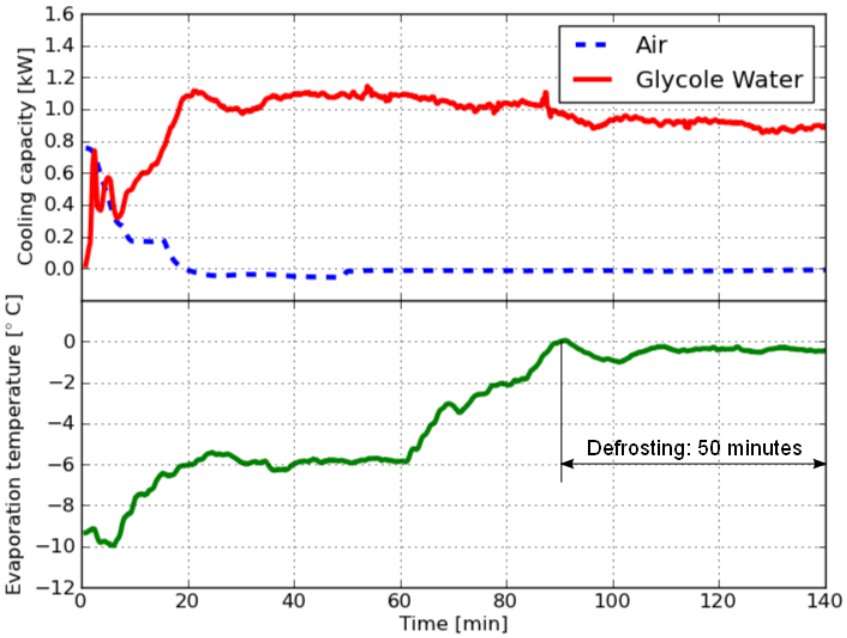

Figure 6: Time series data of the frosted evaporator.

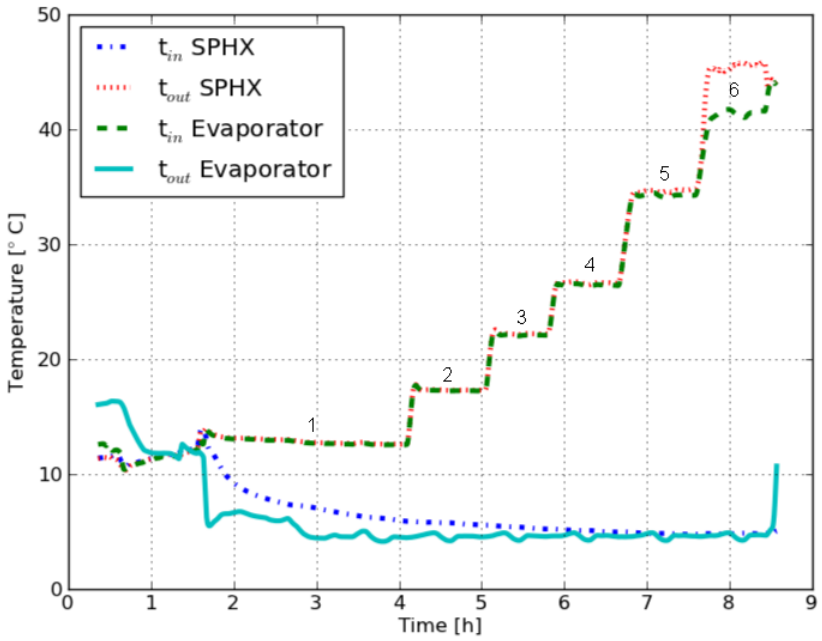

Figure 7: Time series of the four temperatures at inlet and outlet of the SPHX (t_{in} SPHX and t_{out} SPHX) and the evaporator as condenser within the NC cycle (t_{in} Evap and t_{out} Evap). The numbers represent different states of the NC cycle.

The calculation was roughly made by summing up the inner volumes of the circuit which were filled at high pressures (p > 1.8 MPa). In the following are some details on the charging procedures provided: it can be assumed that the state of the refrigerant was liquid at all times during this charging procedure. With the detailed knowledge of temperature and pressure the mass is calculated.

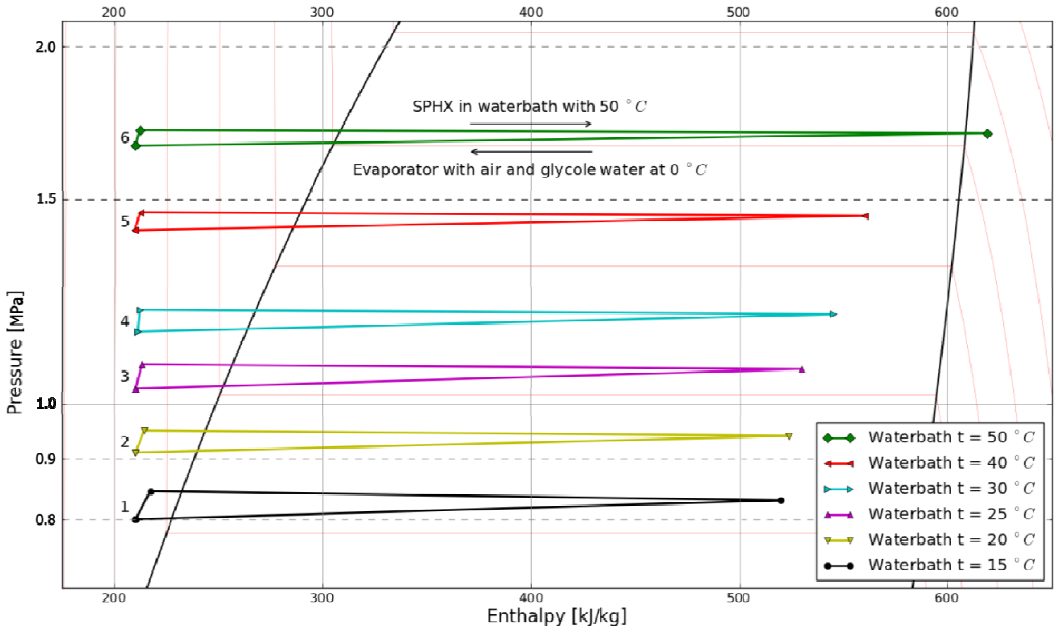

Figure 8: Exemplary experimental NC cycle. The diagram of R1270 is created with Refprop (Lemmon et al. 2010).

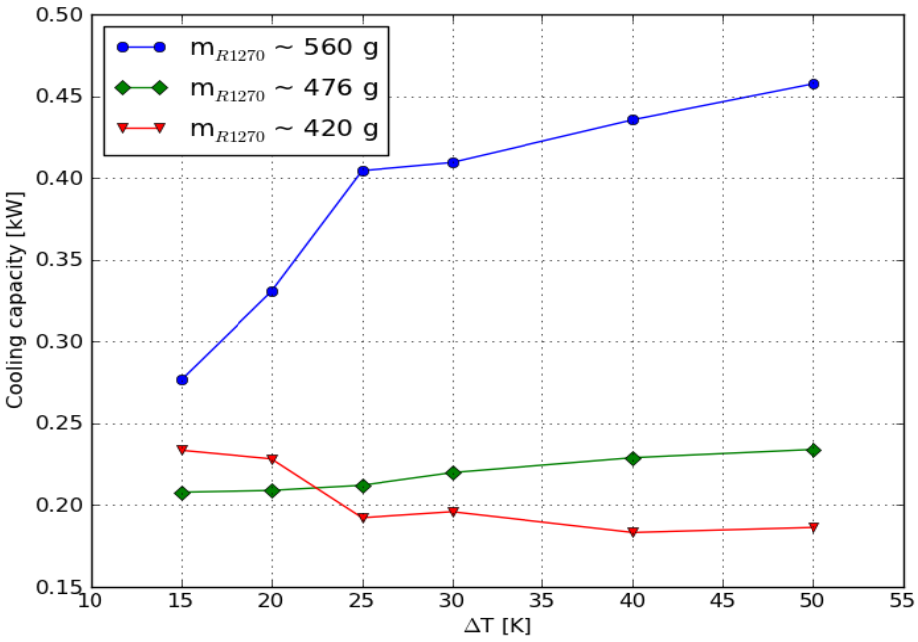

Figure 9: Condensing capacity at different temperature potentials. This figure is based on the time series data presented in figure 7 and some analogous follow-up experiments. The heat source temperatures are held constant at the level of the freezing point.

When analyzing figure 9 and having in mind the characteristics of NC systems as shown in figure 5 the measured states in figure 7 do not represent the maximum possible defrosting capacity.

6 CONCLUSION

A review on flow distribution systems for evaporators was presented in this work. The heat exchanger was applied on an extended test bench for air-driven evaporators now in condition to investigate NC defrosting. The review has shown that with small effort a powerful non-electric defrosting technique can be designed and operated to reduce the demand in electrical energy in comparison to reverse cycle defrosting with reference to Table 1 of about 50 %. Even in a complex NC system with several horizontal oriented and winded tube sections and a non-optimised refrigerant charge a condensing capacity of 0.45 kW was reached.

In a next phase the NC system will be improved by a controllable charge and capacity system to quickly change the system setup, measure precisely the used refrigerant charge and to simplify testing conditions for the defrosting. Subsequently more comprehensive defrosting experiments will be reviewed to enable the generation of stability maps further analysis in the future and more specific design criteria relevant for our system and for natural circulation in heat pumps in general.

The heat exchanger will be further investigated and rebuilt in a second generation, equipped with high dynamic pressure sensors to analyse the fluid distribution on a more basic level at every relevant position to gain broader knowledge and reliability in future design tasks for evaporators. Thus in this way a deeper insight is also possible for the design issues of NC systems. Investigation for the heat exchangers usability within solar-assisted heat pump system has already begun and will be presented in the near future.

7 ACKNOWLEDGEMENTS

This work was enabled by the financial support of the Fraunhofer Society, by the build-up of HP and evaporator laboratory at Fraunhofer ISE. Furthermore, the authors thank all present and former associates who greatly supported the design, construction, commissioning and experimental phase of this work. Last but not least we want to acknowledge the great work of the developers of the open source software Inkscape, Python and the Python module Matplotlib (Hunter 2007).

8 REFERENCES

Bassiouny, M. K., Martin, H. 1984. “Flow distribution and pressure drop in plate heat exchangers - U-type arrangement“, CHEM ENG SCI, Vol. 39, 1984, pp. 693-700.

Bertsch S., Ehrbar M., Hubacher P. 2002. “Verbesserung des Abtauens bei luftbeaufschlagten Verdampfern – Phase 2 – Bewertung der Abtauprozesse“, Final Report, Bern, Switzerland.

Bulletin 20-10 2009. “Sporlan Refrigerant Distributors”, Parker Hannifin, Sporlan Division, Washington, Missouri, USA.

Chawla, Schmitz 1977. “Verfahren und Vorrichtung zur Aufteilung eines stroemenden Flüssigkeits-Gas-Gemisches in mehrere Teilstroeme“, Kueba Kuehlerfabrik, Baierbrunn, Germany. Patent DE2731279.

Hecking B., Russ C., Miara M., Platt M. 2008. “Einsatz von Waermepumpen im Gebaeudebestand – Uebersicht und erste Ergebnisse aus einem Feldtestmonitoring“, 6. Waermepumpenforum, Berlin, Germany.

Hunter, J. D. 2007. “Matplotlib: A 2D Graphics Environment”. COMPUT SCI ENG, Vol. 9, pp. 90-95.

Kew P., Cornwell K., 1997. “Correlation for prediction of boiling heat transfer in small diameter channels“, APPL THERM ENG, Vol. 17, pp. 705-715.

Lemmon, E. W., Huber, M. L., and McLinden, M. O. 2007. “NIST Standard Reference Database 23: Reference Fluid Thermodynamic and Transport Properties-REFPROP”, Version 8.0 National Institute of Standards and Technology, Standard Reference Data Program, Gaithersburg.

Mader G., Thybo C., Larsen L. F. S. 2010. “A METHOD OF CONTROLLING OPERATION OF A VAPOUR COMPRESSION SYSTEM“, Danfoss, Nordborg, Denmark. Patent WO2010/118745 A2. Picture taken from Danfoss North America.

Miara M., Kramer T., Kaczmarek L., Russ C., Guenther D. 2010. „Waermepumpen-Effizienz“, BMWi Project 0327401A, Germany.

Mildenberger J. 2008. “Aufbau eines Pruefstandes zur Untersuchung der Vereisungsproblematik einer CO_2-Luft/Wasser-Waermepumpe mit Naturumlaufabtauung“, Diploma Thesis, TU Brunswik, Germany.

Owens 1971. “Refrigerant Distributor“. Sporlan Valve Company, Missouri, USA. Patent US3563055.

Reichelt J. Year not known. “Instruction and Education Material for Refrigerant Engineers”, TWK Karlsruhe, Germany.

Revellin R., Haberschill P. 2009. “Prediction of frictional pressure drop during flow boiling of refrigerants in horizontal tubes: Comparison to an experimental database“, INT J REF, Vol. 32, pp. 487-497.

Thome J. R. 2004. “Boiling in microchannels: a review of experiment and theory“, INT J HEAT FLUID FL, Vol. 25, pp. 128-139.

Tilney 1957. “Refrigerant Distributor“. Alco Valve Company, Missouri, USA. Patent US2803116.

Wellig B., Imholz M., Albert M. and Hilfiker K. 2008. “DEFROSTING THE FIN TUBE EVAPORATORS OF AIR/WATER HEAT PUMPS USING AMBIENT AIR“, IEA Heat Pump Conference, Zurich, Switzerland.